

Supporting Information

A Universal Strategy for Synthesis of Transition Metal Single Atom Catalysts toward Electrochemical CO₂ Reduction

Bowen Li^a, Yan Liang^b and Yinlong Zhu^{*a}

^a Institute for Frontier Science, Nanjing University of Aeronautics and Astronautics, Nanjing 210016, China. Email: zhuyl1989@nuaa.edu

^b HRL Technology Group, Mulgrave, Victoria 3170, Australia

Experimental Section	Pages S2-S3
Supporting Figures and Tables	Pages S4-S10

Experiment session

Materials. All the solvents and chemicals were available from suppliers and used as received unless specially stated. Dicyandiamide (DCDA, 99%), Dopamine hydrochloride, $\text{NH}_3 \cdot \text{H}_2\text{O}$ (Poison, 28%), ethanol (99%), Iron(III) nitrate nonahydrate ($\text{Fe}(\text{NO}_3)_3 \cdot 9\text{H}_2\text{O}$, 98%), Cobalt(II) nitrate hexahydrate ($\text{Co}(\text{NO}_3)_2 \cdot 6\text{H}_2\text{O}$, 98%), Nickel(II) nitrate hexahydrate ($\text{Ni}(\text{NO}_3)_2 \cdot 6\text{H}_2\text{O}$, 98.5%), Copper(II) nitrate trihydrate ($\text{Cu}(\text{NO}_3)_2 \cdot 3\text{H}_2\text{O}$, 99%), Zinc nitrate hexahydrate ($\text{Zn}(\text{NO}_3)_2 \cdot 6\text{H}_2\text{O}$, 98%), Chromium(III) nitrate nonahydrate ($\text{Cr}(\text{NO}_3)_3 \cdot 9\text{H}_2\text{O}$, 99%), Manganese sulfate monohydrate ($\text{MnSO}_4 \cdot \text{H}_2\text{O}$, Premium), Scandium(III) nitrate hydrate ($\text{Sc}(\text{NO}_3)_3 \cdot x\text{H}_2\text{O}$ was synthesized from fully evaporating solution of dissolved Sc_2O_3 in concentrated HNO_3).

Synthesis of PDA-M (M=Sc, Cr, Mn, Fe, Co, Ni, Cu, Zn): Ammonia aqueous solution (2 ml) was mixed with ethanol (36 ml) and water (94 ml) under stirring for 30 mins. Different metal source (0.02 mmol) and Dopamine hydrochloride (0.003 mol) were dissolved in the mixture of water (6ml) and ethanol (4ml), and then injected into the above mixture solution. The reaction proceeded 24 h with stirring at room temperature. The PDA-M nanospheres were obtained and washed for 3 times by centrifugation with ethanol and dried at 60 °C overnight. For Ni/N-C-HL sample, 0.2 mmol of nickel nitrate was used.

Synthesis of M/N-C: The samples PDA and PDA-M (10mg) mixed with DCDA (100 mg) by milling, then the mixed powder was put into tube furnace and heated slowly from room temperature to 800 °C at 5 °C/min heating rate and then kept at the temperature for 2 h under flowing argon gas, respectively. The furnace cooled down to room temperature naturally in an argon atmosphere. The resultant black carbon material (M/N-C) were washed with 2 M HCl solution to remove nanoparticle aggregates.

CO₂ reduction electrolysis and product analysis

Electrolysis was performed in a gas-tight two-compartment electrochemical cell with a glass frit as the separator. Each compartment contained 10 mL electrolyte and approximately 22.5 mL headspace. To prepare the working electrode, the catalyst (3 mg) and Nafion solution (40 mL) were dispersed in 0.5 mL water and 0.5 mL ethanol by sonicating for 0.5 h to form a homogeneous ink. A graphite rod counter electrode, a Ag/AgCl (3 M KCl) reference electrode and a modified glassy carbon plate (0.3 cm by 1.4 cm, loaded with 30 mL catalyst ink) working electrode were used. Before electrolysis, the cell was degassed by bubbling CO₂ gas for at least 30 min. Exhaust product gas were analysed via online gas chromatography to quantify product distribution.

Characterization

X-ray Diffraction (XRD) data were collected with a Bruker D2 PHASER powder diffractometer (Cu K α radiation, $\lambda = 0.15406$ nm). Texture properties and specific surface areas were evaluated with N₂-

sorption technique (Micromeritics APSP 2460). Transmission electron microscopic (TEM) images were collected on a FEI Tecnai G2 F20 TEM. Scanning electron microscopic (SEM) images were recorded on a FEI Magellan 400 FEG SEM equipped with Bruker Quantax 400 X-ray analysis system. Gas chromatography (GC) was performed with an Agilent 7820 A gas chromatography system equipped with a HP-PLOT MoleSieve (5A) column and a thermal conductivity detector (TCD). The carrier gas was helium (99.99%) for CO analysis while nitrogen (99.99%) was used as carrier gas for H₂ analysis. The retention times were compared with those of known compounds. All the electrochemical experiments were conducted on a CHI 760D electrochemical workstation (CHI Instruments, Austin, Texas, USA) at room temperature (22 ± 2 °C).

Supporting Figures

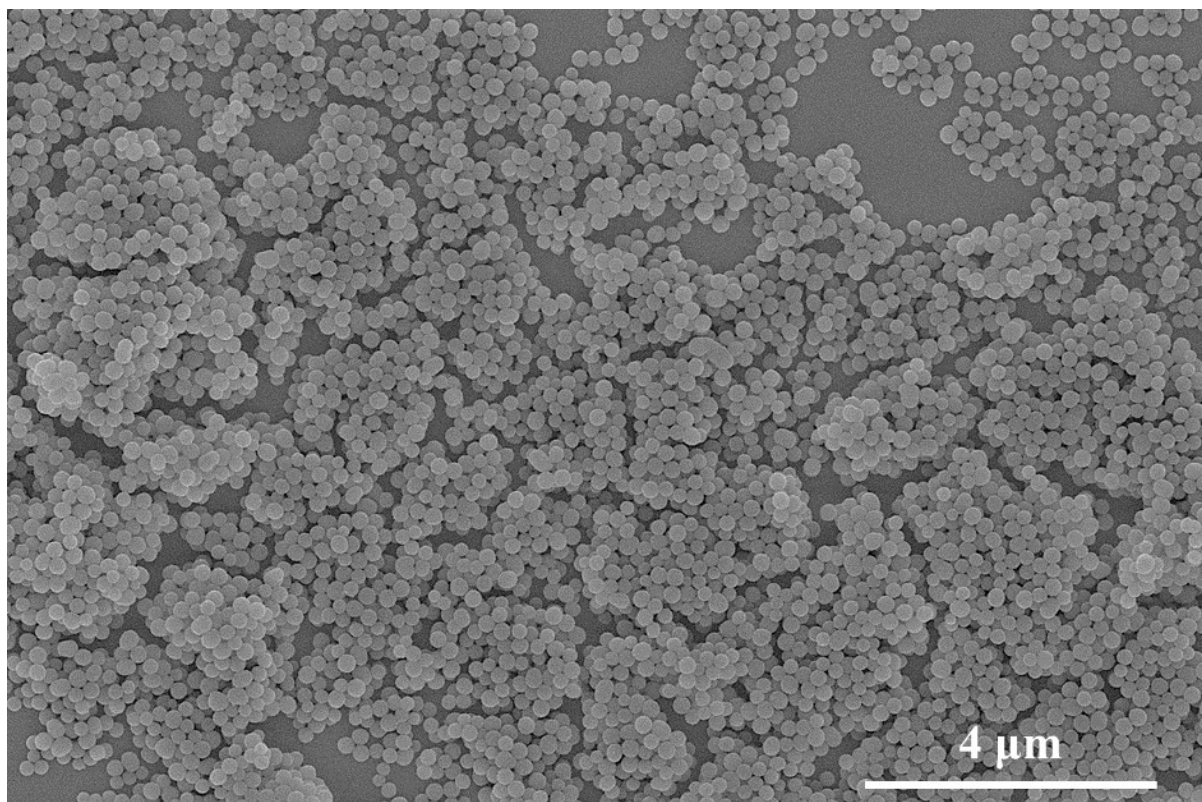


Figure S1. Representative SEM image of PDA-Ni at lower resolution, to illustrate the homogeneity of spherical morphology.

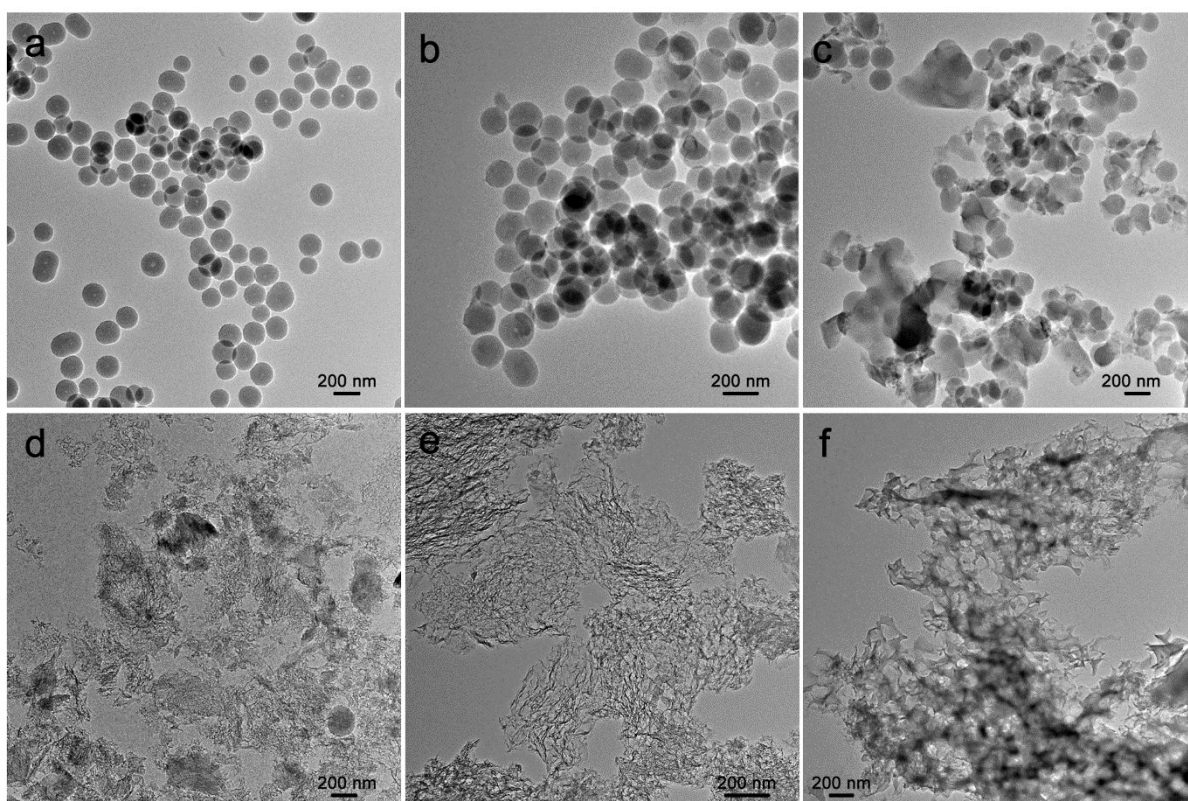


Figure S2. Representative TEM images of mixing PDA-Ni with increasing concentrations of DCDA. (a) was TEM images when pyrolysis of PDA-Ni take place in absence of DCDA, and the sample remained in spherical shape. PDA-Ni to DCDA ratio then increases from 0.5 (b), 1.0 (c), 5.0 (d) to 10.0 (e and f), while the spherical shape has been gradually transformed into nanosheets.

To better understand the role of DCDA in the formation of M/N-C samples, control experiments were conducted with varied DCDA to PDA-Ni ratio. Without the presence of DCDA, PDA-Ni polymers maintained nanosphere shape after pyrolysis, as shown in the TEM images. After adding DCDA to PDA-Ni polymers, the formation of carbonaceous nanosheets becomes gradually obvious with increasing ratio of DCDA in the mixture. In addition to acting as nitrogen source, it is believed that DCDA played a key role in the process for forming carbonaceous nanosheet support. The mechanism can be ascribed to that adhesive DCDA on the surface of PDA-Ni nanospheres could exfoliate the nanospheres into nanosheets, by reaction between the phenolic hydroxyl groups of PDA and the amino groups of DCDA.¹

1. Y. Liang, H. Zhang, J. Zhang, X. Cheng, Y. Zhu, L. Luo, S. Lu, J. Wei, H. Wang, *Electrochim. Acta* 2019, 135397.

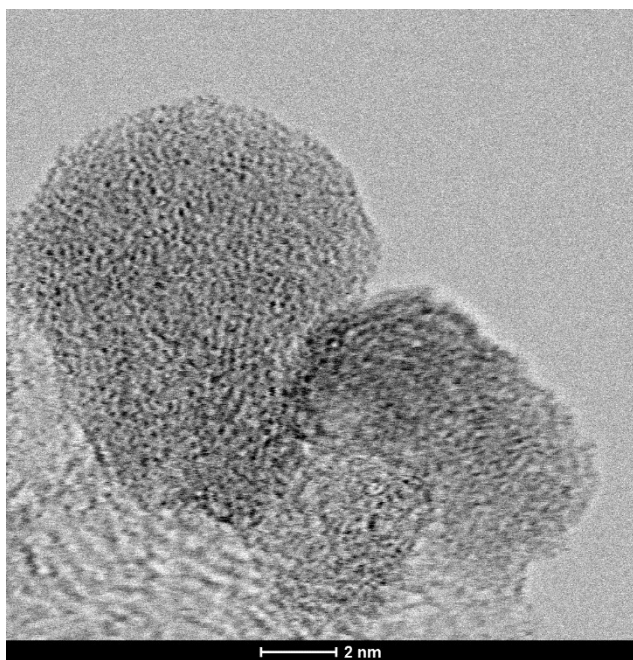


Figure S3. Representative high resolution bright field TEM image of Ni/N-C taken with AC-TEM, corresponding to the AC-STEM image presented in manuscript Figure 1d.

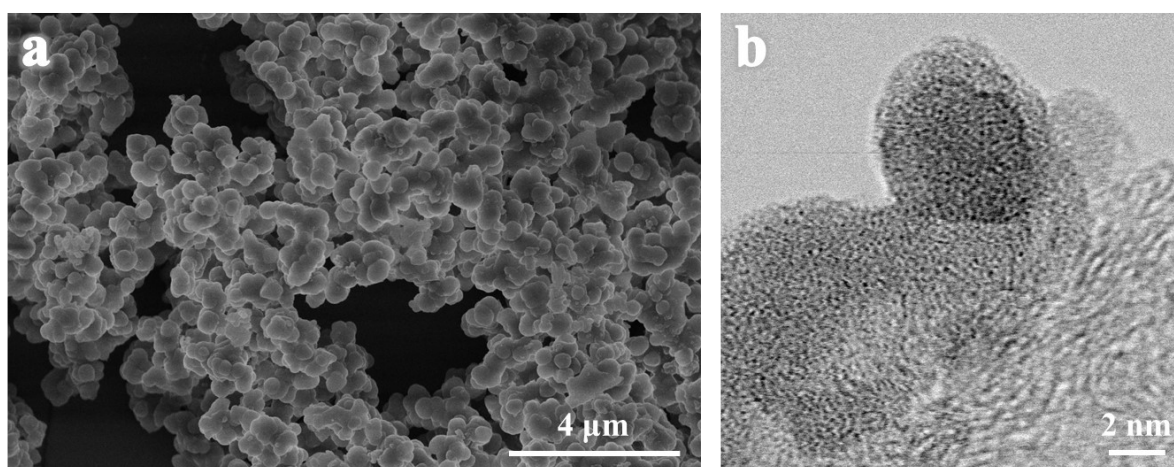


Figure S4. Representative (a)SEM image of PDA-Ni precursor and (b) HRTEM image of Ni/N-C-HL at 10 times increased Ni loading, to illustrate the atomic dispersion of Ni at increased loading.

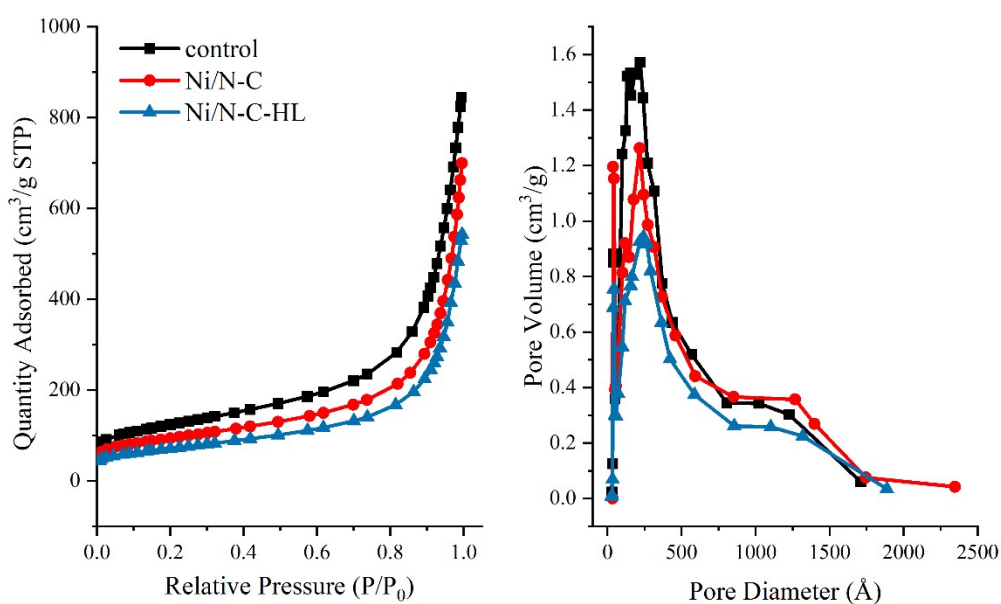


Figure S5. (a) N₂-isotherm and (b) BJH Pore size distribution plot of Ni/N-C and Ni/N-C-HL samples. Control sample was obtained by direct pyrolysis of PDA/DCDA mixture without pre-installed Ni ions.

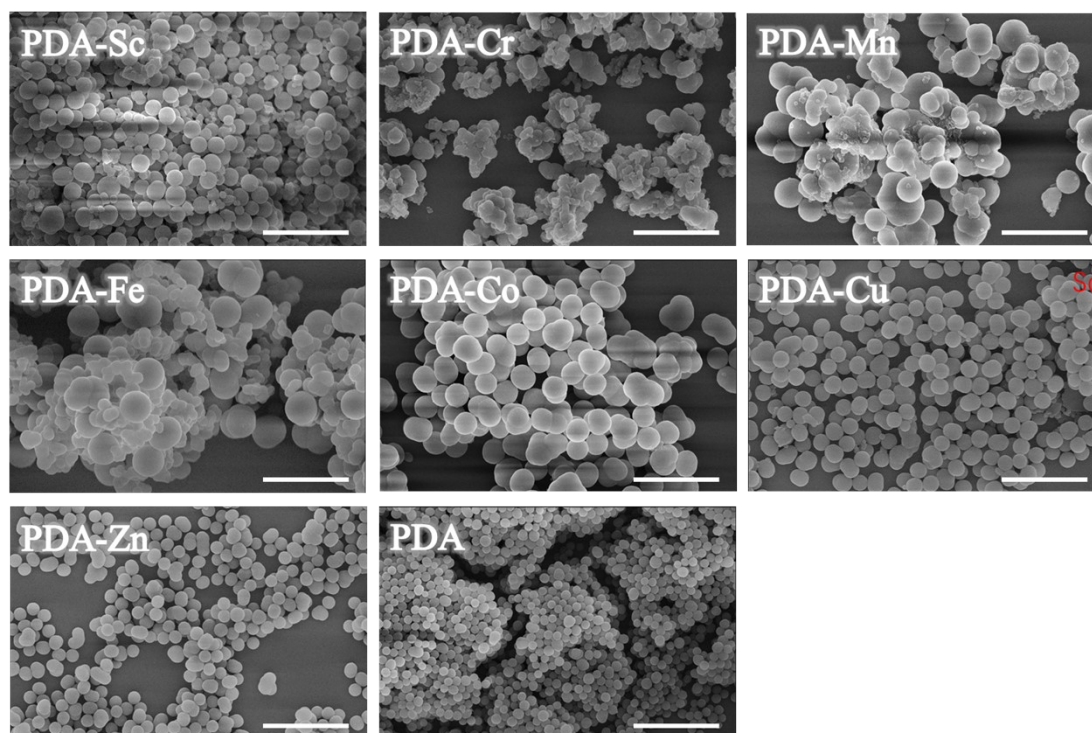


Figure S6. Representative SEM images of various PDA-M samples, prepared by replacing nickel nitrate with different metal salts. The last PDA sample was prepared without adding metal salt solution.

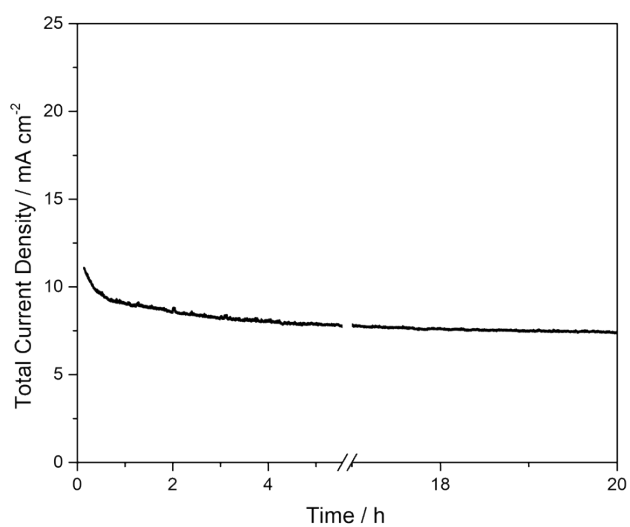


Figure S7. eCO₂RR stability test evaluated using Ni/N-C sample.

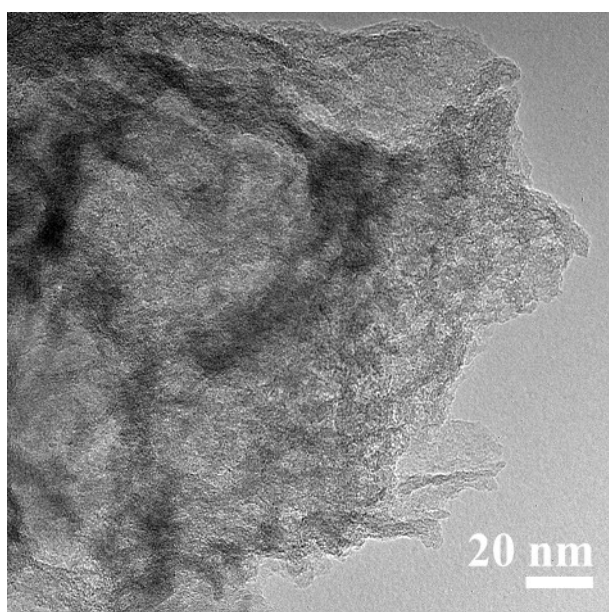


Figure S8. Representative TEM image of Ni/N-C sample after 20 h stability test.

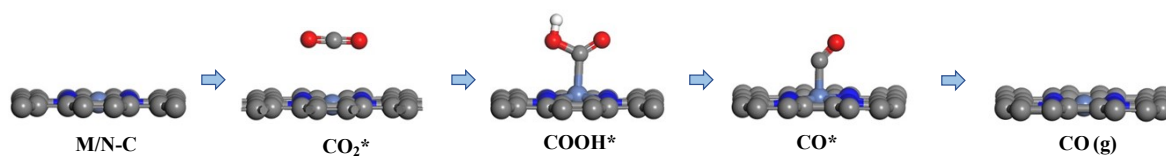


Figure S9. Elementary steps illustrating the electrochemical conversion of CO₂ to CO.

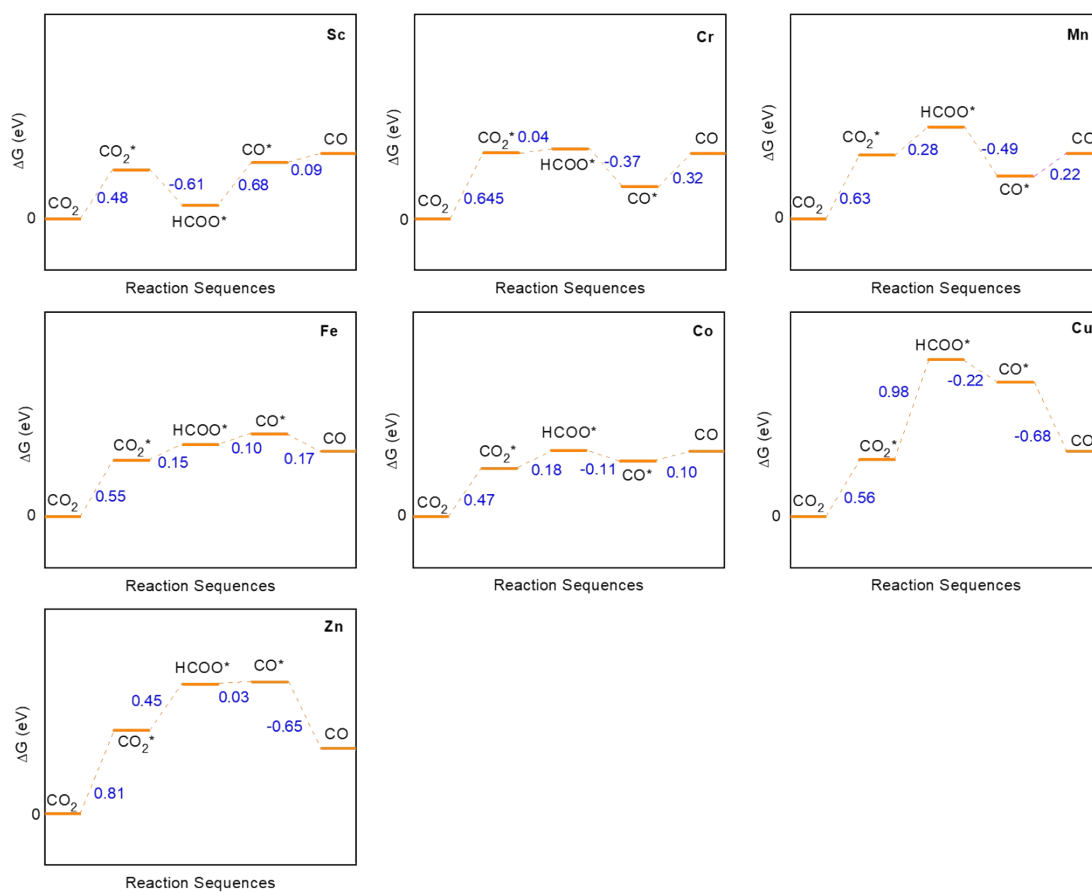


Figure S9. Free energy diagrams of eCO₂RR to CO over different M/N-C catalysts.

Table S1. Detailed reaction data on eCO₂RR over Ni/N-C catalysts. All reactions are carried out using 0.5 M KHCO₃ electrolyte in a H-cell setup. Error bar data were obtained by repeating the same reaction 3 times.

Entry	Applied Potential V (vs. RHE)	FE _{CO} (%)	Partial current j_{co} (mA cm ⁻²)	FE _{H₂} (%)	Partial current j_{H_2} (mA cm ⁻²)
1	-0.4	12.4±0.62	0.0868±0.00434	83.4±4.17	0.5838±0.0292
2	-0.45	34.6±1.73	0.346±0.0173	66.6±3.33	0.666±0.0333
3	-0.55	81.4±4.07	2.52±0.126	26±1.55	0.806±0.0403
4	-0.65	99.3±4.97	8.34±0.417	10±0.50	0.84±0.0420
5	-0.75	97.6±4.88	14.6±0.732	6.8±0.34	1.02±0.0510
6	-0.85	101±5.05	22.2±1.11	6.2±0.31	1.364±0.0682
7	-0.95	97.6±4.88	26.3±1.32	5.6±0.28	1.512±0.0756
8	-1.05	90.3±4.52	29.8±1.49	7.9±0.40	2.607±0.130

Table S2. Detailed reaction data on eCO₂RR over all M/N-C catalysts. All reactions are carried out using 0.5 M KHCO₃ electrolyte in a H-cell setup.

V (vs. RHE)	Zn/N-C		Cu/N-C		Ni/N-C		Co/N-C		Fe/N-C		Mn/N-C		Cr/N-C		Sc/N-C	
	FE _{CO} (%)	j_{co} (mA cm ⁻²)	FE _{CO} (%)	j_{co} (mA cm ⁻²)	FE _{CO} (%)	j_{co} (mA cm ⁻²)	FE _{CO} (%)	j_{co} (mA cm ⁻²)	FE _{CO} (%)	j_{co} (mA cm ⁻²)	FE _{CO} (%)	j_{co} (mA cm ⁻²)	FE _{CO} (%)	j_{co} (mA cm ⁻²)	FE _{CO} (%)	j_{co} (mA cm ⁻²)
-0.4	N.A.	N.A.	N.A.	N.A.	12.4	0.0868	N.A.	N.A.	N.A.	N.A.	N.A.	N.A.	N.A.	N.A.	N.A.	N.A.
-0.45	N.A.	N.A.	N.A.	N.A.	34.6	0.346	1.0	1.16	N.A.	N.A.	N.A.	N.A.	N.A.	N.A.	N.A.	N.A.
-0.55	11	0.054	11	0.078	81.4	2.52	2.2	3.16	55	0.117	29	0.0833	21	0.257	15	0.413
-0.65	8.3	0.083	12	0.19	99.3	8.34	2.8	5.34	48	0.224	25	0.187	15	0.504	24	1.16
-0.75	4.0	0.14	13	0.46	97.6	14.6	4.3	7.34	41	0.373	22	0.376	11	1.10	26	1.81
-0.85	5.9	0.35	11	0.67	101	22.2	4.7	7.62	29	0.425	22	0.690	12	1.50	27	2.79
-0.95	4.5	0.27	6.8	0.75	97.6	26.3	5.2	7.31	22	0.548	20	0.767	9.7	2.08	15	3.14
-1.05	N.A.	N.A.	5.7	0.91	90.3	29.8	4.6	7.48	17	0.576	18	0.494	7.2	2.15	5.0	3.81